

HUMAN GENETICS

Pathogenic variants in *SMARCA5*, a chromatin remodeler, cause a range of syndromic neurodevelopmental features

Dong Li^{1,*†}, Qin Wang^{2†}, Naihua N. Gong³, Alina Kurolap⁴, Hagit Baris Feldman^{4,5}, Nikolas Boy⁶, Melanie Brugger^{7,8}, Katheryn Grand⁹, Kirsty McWalter¹⁰, Maria J. Guillen Sacoto¹⁰, Emma Wakeling¹¹, Jane Hurst¹¹, Michael E. March¹, Elizabeth J. Bhoj¹, Małgorzata J. M. Nowaczyk¹², Claudia Gonzaga-Jauregui¹³, Mariam Mathew¹⁴, Ashita Dava-Wala¹⁴, Amy Siemon¹⁵, Dennis Bartholomew¹⁵, Yue Huang¹⁶, Hane Lee¹⁷, Julian A. Martinez-Agosto¹⁶, Eva M. C. Schwaibold¹⁷, Theresa Brunet⁷, Daniela Choukair¹⁹, Lynn S. Pais²⁰, Susan M. White^{21,22}, John Christodoulou^{21,22}, Dana Brown²³, Kristin Lindstrom²³, Theresa Grebe^{23,24}, Dov Tiosano^{25,26}, Matthew S. Kayser³, Tiong Yang Tan^{21,22}, Matthew A. Deardorff²⁷, Yuanquan Song^{2,28*}, Hakon Hakonarson^{1,29}

Intellectual disability encompasses a wide spectrum of neurodevelopmental disorders, with many linked genetic loci. However, the underlying molecular mechanism for more than 50% of the patients remains elusive. We describe pathogenic variants in *SMARCA5*, encoding the ATPase motor of the ISWI chromatin remodeler, as a cause of a previously unidentified neurodevelopmental disorder, identifying 12 individuals with de novo or dominantly segregating rare heterozygous variants. Accompanying phenotypes include mild developmental delay, frequent postnatal short stature and microcephaly, and recurrent dysmorphic features. Loss of function of the *SMARCA5* *Drosophila* ortholog *Iswi* led to smaller body size, reduced sensory dendrite complexity, and tiling defects in larvae. In adult flies, *Iswi* neural knockdown caused decreased brain size, aberrant mushroom body morphology, and abnormal locomotor function. *Iswi* loss of function was rescued by wild-type but not mutant *SMARCA5*. Our results demonstrate that *SMARCA5* pathogenic variants cause a neurodevelopmental syndrome with mild facial dysmorphism.

INTRODUCTION

Regulation of gene expression by transcription requires a highly coordinated and precise process that involves chromatin regulators and modifiers, transcription factors, cohesins, and mediators. The basic and dynamic unit of chromatin is the nucleosome, onto which DNA is wrapped around an octameric histone complex. Subsequent high-order DNA structure requires chromatin remodelers to make DNA accessible to alter nucleosome position and, in turn, regulate gene transcription using the energy released by adenosine triphosphate (ATP) hydrolysis. ATP-dependent nucleosome remodeling not only provides an open and accessible chromatin state but also is involved in chromatin assembly, nucleosome sliding and spacing, and gene

repression, which are crucial for a wide range of biological processes in normal development including early embryonic development stages (1). ATP-dependent nucleosome remodelers, which share similar adenosine triphosphatase (ATPase) domains and have an affinity to the nucleosome, are categorized into four subfamilies based on their unique domains and associated subunits: SWI/SNF, ISWI (imitation switch), CHD (chromatin helicase DNA binding), and INO80/SWR1.

A number of neurodevelopmental disorders have been linked to pathogenic variants in genes encoding chromatin remodelers and associated subunits, including the SWI/SNF subunits ARID1A [Mendelian Inheritance in Man (MIM): 603024], ARID1B (MIM: 614556), ARID2 (MIM: 609539), SMARCA4 (MIM: 603254), SMARCB1

¹Center for Applied Genomics, Children's Hospital of Philadelphia, Philadelphia, PA, USA. ²Raymond G. Perelman Center for Cellular and Molecular Therapeutics, Children's Hospital of Philadelphia, Philadelphia, PA, USA. ³Department of Psychiatry, Perelman School of Medicine at the University of Pennsylvania, Philadelphia, PA, USA. ⁴The Genetics Institute, Tel Aviv Sourasky Medical Center, Tel Aviv, Israel. ⁵Sackler Faculty of Medicine, Tel Aviv University, Tel Aviv, Israel. ⁶Division of Child Neurology and Metabolic Medicine, Center for Child and Adolescent Medicine, University Hospital Heidelberg, Heidelberg, Germany. ⁷Institute of Human Genetics, Technical University Munich, Munich, Germany. ⁸Institute of Human Genetics, University Hospital LMU Munich, Goethestr. 29, Munich, Germany. ⁹Department of Pediatrics, Cedars-Sinai Medical Center, Los Angeles, CA, USA. ¹⁰GeneDx, Gaithersburg, MD, USA. ¹¹North East Thames Regional Genetic Service, Great Ormond Street Hospital for Children NHS Foundation Trust, London, UK. ¹²Department of Pathology and Molecular Medicine, McMaster University, Hamilton, Ontario, Canada. ¹³Regeneron Genetics Center, Tarrytown, New York, NY, USA. ¹⁴Institute for Genomic Medicine, Nationwide Children's Hospital, Columbus, OH, USA. ¹⁵Department of Pediatrics and Clinical Genetics, Nationwide Children's Hospital, Columbus, OH, USA. ¹⁶Department of Human Genetics; Division of Medical Genetics, Department of Pediatrics; David Geffen School of Medicine, University of California, Los Angeles, Los Angeles, CA, USA. ¹⁷Department of Pathology and Laboratory Medicine; Department of Human Genetics; David Geffen School of Medicine, University of California, Los Angeles, Los Angeles, CA, USA. ¹⁸Institute of Human Genetics, Heidelberg University, Heidelberg, Germany. ¹⁹Division of Paediatric Endocrinology and Diabetes, Department of Paediatrics, University Hospital Heidelberg, Heidelberg, Germany. ²⁰Broad Center for Mendelian Genomics, Program in Medical and Population Genetics, Broad Institute of Massachusetts Institute of Technology and Harvard, Cambridge, MA, USA. ²¹Victorian Clinical Genetics Services, Murdoch Children's Research Institute, Melbourne, Australia. ²²Department of Paediatrics, University of Melbourne, Melbourne, Australia. ²³Division of Genetics and Metabolism, Phoenix Children's Hospital, Phoenix, AZ, USA. ²⁴College of Medicine, University of Arizona, Phoenix, 475 N. 5th Street, Phoenix, AZ, USA. ²⁵Pediatric Endocrinology Unit, Ruth Rappaport Children's Hospital, Rambam Healthcare Campus, Haifa, Israel. ²⁶The Ruth and Bruce Rappaport Faculty of Medicine, Technion, Israel Institute of Technology, Haifa, Israel. ²⁷Departments of Pathology and Pediatrics, Children's Hospital Los Angeles, and University of Southern California, Los Angeles, CA, USA. ²⁸Department of Pathology and Laboratory Medicine, University of Pennsylvania, Philadelphia, PA, USA. ²⁹Department of Pediatrics, University of Pennsylvania Perelman School of Medicine, Philadelphia, PA, USA.

*Corresponding author. Email: lid2@email.chop.edu (D.L.); songy2@email.chop.edu (Y.S.)

†These authors contributed equally to this work.

(MIM: 601607), SMARCE1 (MIM: 603111), SMARCD1 (MIM: 601735), SMARCC2 (MIM: 601734), and DPF2 (MIM: 601671) in Coffin-Siris syndrome (2–8); SMARCA2 (MIM: 600014) in Nicolaides-Baraitser syndrome (MIM: 601358) (9, 10); BCL11A (MIM: 606557) in Dias-Logan syndrome (MIM: 617101) (11); ACTL6B in intellectual developmental disorder with severe speech and ambulation defects (MIM: 618487) (12); ACTB (MIM: 102630) and ACTG1 (MIM: 102560) in Baraitser-Winter syndrome (13); CHD subunits CHD4 (MIM: 603277) in Sifrim-Hitz-Weiss syndrome (MIM: 617159) (14, 15); CHD7 (MIM: 608892) in CHARGE syndrome (MIM: 214800) (16); CHD3 (MIM: 602120) in Snijders Blok-Campeau syndrome (MIM: 618205) (17); ISWI subunits BPTF (MIM: 601819) in neurodevelopmental disorder with dysmorphic facies and distal limb anomalies (18); and, last, SMARCA1 in Coffin-Siris syndrome-like and Rett syndrome-like phenotypes (19, 20).

ISWI is one of the well-studied chromatin remodeling complexes in animal models. Iswi was first identified in *Drosophila melanogaster*, which has a single Iswi ATPase motor protein compared to two in humans (21–23). In vertebrates, the ISWI complex is typically composed of two to four subunits, including an ATPase, a catalytic subunit, and a scaffolding component involved in target recognition or stabilization. Eight different ISWI-containing chromatin remodeling complexes have been identified in humans, including ACF, CHRAC, NoRC, RSF, WICH, SNF2H/NURD/Cohesin, CERF, and NURF (24–31). All of these complexes contain either the SNF2L or SNF2H ATPase subunit encoded by *SMARCA1* or *SMARCA5*, respectively. The two proteins share 83% amino acid similarity, and they are interchangeable in these complexes (32). Morpholino knockdown of the zebrafish *SMARCA5* ortholog results in decreased body size and reduced cardiac ventricle size (33). A critical role for *SMARCA5* in mammalian development has also been demonstrated in mice, where knockout embryos die during preimplantation stages and conditional knockouts lead to substantial reductions in body weight, body size, and brain size with cerebellar hypoplasia (34). However, a specific syndrome associated with *SMARCA5* rare germline variants has not yet been described. In addition, whereas *SMARCA5* has been implicated in neural stem cell proliferation and differentiation (26, 34, 35), the spectrum of its functions in the nervous system remains undetermined, with the underlying mechanisms largely underexplored.

Here, we report 12 individuals (6 females and 6 males) from 10 unrelated families assembled through international collaborations with germline variants in *SMARCA5*. These individuals share the core presentations of mild developmental delay, postnatal microcephaly, short stature, and mild facial dysmorphism. Using a *Drosophila* model, we found that Iswi loss-of-function (LoF) results in a spectrum of neurodevelopmental abnormalities including reduced body/brain size, dendrite and axon mispatterning, and behavioral deficits. These findings mirror the key growth and cognitive phenotypes present in affected individuals. More importantly, human wild-type (WT) *SMARCA5* but not affected individuals' variants rescue these phenotypes, confirming their pathogenic role in these models. Together, these data describe a novel syndromic neurodevelopmental disorder caused by pathogenic variants in the *SMARCA5* gene.

RESULTS

Clinical presentations of individuals with *SMARCA5* variants

After identifying de novo or dominantly inherited variants in *SMARCA5* in each family, we assembled the cohort of 12 individuals

through the assistance of GeneMatcher (36). Individual 3 was recruited from the Deciphering Developmental Disorders (DDD) study. Clinical phenotypes overlapped and are summarized in Table 1, and detailed data are compiled in table S1. The majority of the probands (8 of 10; 80%) had neurodevelopmental disorders with developmental delays in some area, but most delays were mild. Because detailed developmental history information was inadequate for the two adult individuals (mother and maternal grandmother of individual 4), their degree of neurodevelopmental delay is unclear. While all probands have normal hearing, mild ($N = 4$) or severe ($N = 2$) speech delay was present in six probands (60%; 6 of 10), with the age of first words ranging from 12 to 27 months. Motor delay was reported in six probands (60%), with the age of walking ranging from

Table 1. Summary of clinical characteristics associated with heterozygous *SMARCA5* variant.

Clinical findings	Number of individuals/assessed	Percentage
Gender	6 female and 6 male	
Neurodevelopment		
Prenatal microcephaly	3/7	43%
Postnatal microcephaly	9/12	75%
Postnatal short stature	10/12	83%
Failure to thrive	8/10	80%
Hypotonia	5/10	50%
Developmental delays	8/10	80%
Motor delay	6/10	60%
Speech/language delay	6/10	60%
Behavioral problems	3/10	30%
Facial feature		
Blepharophimosis/short palpebral fissures	9/11	82%
Epicanthal folds	4/11	36%
Periorbital fullness	8/9	89%
Wide/prominent nasal bridge	8/9	89%
Short/smooth philtrum	8/10	80%
Thin or tented upper lip	8/10	80%
Broad, arched, sparse, or horizontal eyebrows	11/11	100%
Prominent ears or attached ear lobes	9/10	90%
Other abnormalities		
Limb abnormalities	10/11	91%
Eye/vision	5/12	42%
Seizures	2/12	17%

15 to 48 months. Hypotonia was found in five probands (50%), and peripheral hypertonia was noted in individual 4 during infancy. Regarding cognition, four probands had mild intellectual disability and one had severe intellectual disability (50%). A formal diagnosis of autism spectrum disorder was made in only individual 3, and attention deficit disorder/attention-deficit/hyperactivity disorder was detected in three probands (30%). A brain magnetic resonance imaging scan was performed for seven probands and brain computed tomography scan or head ultrasound for two additional probands, showing generally normal morphology, although individual 11 showed mildly delayed myelination and periventricular occipital gliosis and individual 12 showed Chiari malformation type 1. Seizures occurred in two probands (20%). Postnatal microcephaly [head circumference (HC) ≤ -2 SD], short stature (height ≤ -2 SD), and failure to thrive, which were concomitant with feeding difficulties, were present in eight probands (80%), among whom two individuals had birth weight below -2 SD, one had birth length below -2 SD, and three had birth HC less than -2.5 SD. The mother (individual 5) of proband 4 also had short stature and microcephaly when evaluated at age of 39 years old, and her mother (individual 6) also had short stature. Two individuals in the cohort, individuals 10 and 11, had normal postnatal height and weight, with individual 11 having a normal head circumference and individual 10 having macrocephaly. Eight of nine probands in this cohort (89%) had some type of abnormalities of extremities, including brachydactyly (two of five), clinodactyly (three of seven), 2-3 toe syndactyly (two of seven), and hallux valgus/sandal gap (six of seven), whereas cardiac, gastrointestinal, and genitourinary defects were

uncommon (table S1). Individual 2 had multiple cardiac septal defects and a noncompaction dilated cardiomyopathy, with no causative variants in known cardiac genes identified by her clinical exome sequencing. A dermatologic finding, café au lait macule, was identified in two individuals (individuals 3 and 9), who had the recurrent variant, c.1301_1306del, p.(Ile434_Leu435del). Photographs from all participants show a number of shared craniofacial features, including blepharophimosis and/or short palpebral fissures with or without almond-shaped eyes (9 of 11), periorbital fullness (8 of 9), epicanthal folds (4 of 11), a wide/prominent nasal bridge (8 of 9), a short/smooth philtrum (8 of 10), a thin or tented upper lip (8 of 10), broad, arched, sparse, or horizontal eyebrows (11 of 11), and prominent ears or attached ear lobes (9 of 10) (Fig. 1 and table S1). Vision abnormalities are reported in 5 of 12 cases, including myopia, hyperopia, strabismus, and astigmatism. A search of the ClinVar database noted one additional individual (ID 599594) with short stature and a de novo *SMARCA5* variant, c.940A>C, p.(Lys314Gln), although no detailed clinical information was available for this subject. Together, these data indicated that variants in *SMARCA5* are associated with a variable neurodevelopmental phenotype with predominantly mild developmental delay and intellectual disability, short stature, and microcephaly.

Identification of *SMARCA5* variants

Exome sequencing of the 10 families revealed nine different heterozygous novel variants in *SMARCA5* (NM_003601.3), including eight variants confirmed to be de novo in nine individuals. Notably, two unrelated individuals were found to carry the same de novo variant,



Fig. 1. Facial photographs of affected individuals with *SMARCA5* variants showing dysmorphisms. Individual identifiers correlate with those in table S1. Note the similarities in facial appearance with blepharophimosis, short palpebral fissures, periorbital fullness, epicanthal folds, wide and/or high nasal bridge, short and/or flat philtrum, thin upper lip, and arched eyebrows. Individual 1: 3.7-year-old male; individual 4: 18-year-old male; individual 5: 39-year-old female; individual 7: 9.5-year-old female; individual 10: 3-year-old male; individual 11: 3.6-year-old male. Photo credits: M. A. Deardorff, Children's Hospital Los Angeles; A. Kurolap and D. Tiosano, Ruth Rappaport Children's Hospital; M. J. M. Nowaczyk, McMaster University; Y. Huang, University of California, Los Angeles; N. Boy, University Hospital Heidelberg.

c.1301_1306del, p.(Ile434_Leu435del). One missense variant, c.1711G>C, p.(Ala571Pro), was identified in a three-generation pedigree with an affected proband, mother, and maternal grandmother. These nine variants include one splice-altering variant, c.802-2A>G; one in-frame deletion, c.1301_1306del, p.(Ile434_Leu435del); and seven missense variants, c.1130A>T, p.(Asp377Val); c.1682C>A, p.(Ala561Asp); c.1711G>C, p.(Ala571Pro); c.1775G>A, p.(Arg592Gln); c.1855G>C, p.(Glu619Gln); c.2207G>A, p.(Arg736Gln); and c.2677G>A, p.(Glu893Lys) (Fig. 2A). All variants were absent in population genomics resources (i.e., 1000 Genomes Project, ESP6500SI, and gnomAD) and our in-house dataset of >10,000 exomes. All seven missense variants were predicted to be deleterious by multiple bioinformatic prediction algorithms (SIFT, LRT, MutationTaster, CADD, etc.) (table S2). Reverse transcription polymerase chain reaction (RT-PCR) followed by Sanger sequencing of complementary DNA (cDNA) from fibroblasts and a lymphoblastoid cell line (LCL) obtained from individual 1 with the splice-altering variant demonstrated that it causes exon 7 skipping, leading to an in-frame deletion of 52 amino acids (p.Ala268_Lys319del) in the highly conserved ATPase domain (Fig. 2B). These missense variants (including the

ClinVar variant) and the small deletions were mapped to a protein schematic, and eight variants appear to cluster within or around the helicase domains, whereas p.(Arg736Gln) and p.(Glu893Lys) are located in the HAND-SANT-SLIDE (HSS) domains (Fig. 2A). Of note, all the variants reside in protein locations intolerant to change as calculated by the MetaDome server (Fig. 2A and table S2).

To explore the structural impact of the six missense variants within or around the helicase domains, the recently published cryogenic electron microscopy three-dimensional structure (37) of WT SMARCA5 incorporated with the nucleosome complex was obtained [Protein Data Bank (PDB): 6ne3]. SMARCA5 binds to DNA in the nucleosome through its ATPase helicase domains, which form a positively charged cleft on the binding surface (fig. S1A). The p.(Lys314Gln) and p.(Asp377Val) changes result in loss of the positive charge, and the p.(Ala561Asp) change introduces a negatively charged side chain, which may diminish its anchor of DNA binding (table S2 and fig. S1, B and C). Similarly, the p.(Ala571Pro), p.(Arg592Gln), and p.(Glu619Gln) changes may disturb hydrogen bonds and structural stability, therefore possibly affecting interaction with DNA, histone, or adenosine diphosphate (ADP) ligand binding (table S2 and

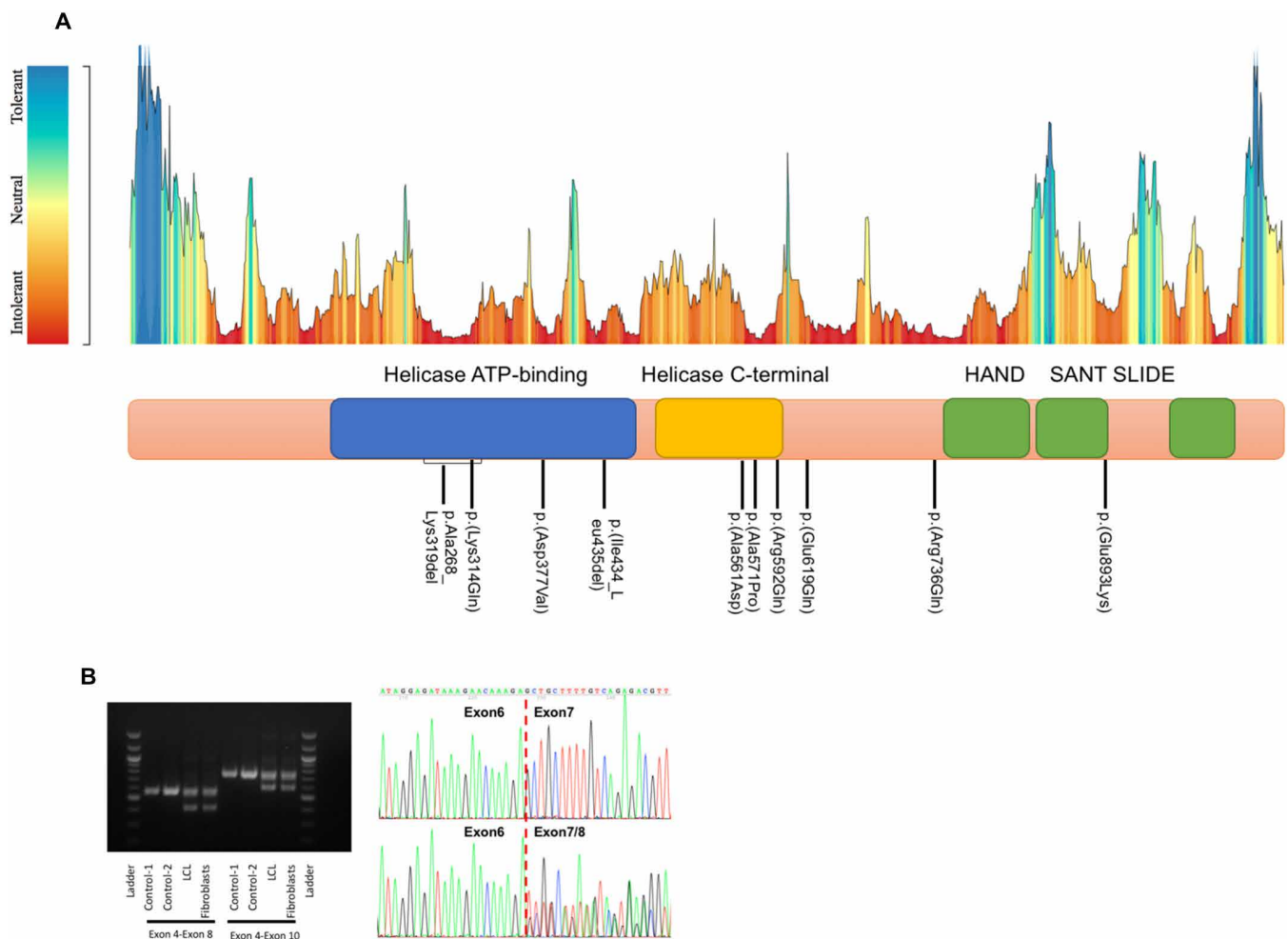


Fig. 2. Molecular genetic findings. (A) An intolerance landscape plot generated by MetaDome for *SMARCA5* variant analysis (top panel) and a schematic outline of *SMARCA5* protein showing conserved variants identified in individuals 1 to 12 and ClinVar at the bottom. (B) RT-PCR analysis of individual 1's fibroblasts and lymphoblastoid cell line showing the *SMARCA5* exon 7 skipping in both cell types because of a splice-altering variant.

fig. S1, B and C). Recent studies have demonstrated that the acidic patch, a negatively charged structure on the surface of the nucleosome, is critically important for recruiting chromatin remodelers, and an acidic patch binding (APB) motif in SMARCA5 has been discovered (38). Notably, the substitution of Arg736, one of the five residues in the APB motif, with alanine in SMARCA5 disrupted its nucleosome sliding activity (39). It seems reasonable to speculate that the replacement of Arg736 with glutamine, similar loss of positive charge, and the side chain changing from a large residue to a small one could similarly alter its remodeler activity. The three-dimensional structure of the HSS domains of WT human SMARCA5 was obtained by using homology modeling with SWISS-MODEL. The x-ray structure of *Drosophila* *Iswi* at a 1.9-Å resolution was used as a template, as it demonstrates 81.25% identity with human SMARCA5 (PDB: 1ofc) (40). As shown in fig. S1D, residue Glu893 was mapped onto the SANT domain helix 3 (SANT3), a recognition helix that makes contacts with unmodified histone tails and has an overall negatively charged surface. A change from a negatively charged side chain to a positively charged one [p.(Glu893Lys)] in the SANT motif, which is predicted to disrupt a local salt bridge, may affect SANT motif substrate recognition ability to contact histone, and, in turn, to hinder ATPase binding.

SMARCA5's ortholog *Iswi* plays a key role in *Drosophila* larval development

To gain independent support for pathogenicity of the variants identified in humans and investigate whether SMARCA5 is required for normal development, we studied the *Drosophila* gene *Iswi* (*Imitation SWI*), which is orthologous to human *SMARCA1* or *SMARCA5*. We first assessed the functional effects of an *Iswi* LoF mutant, *Iswi*², on larvae development (41) and found that *Iswi*² homozygous larvae died before the end of larval stage. For those that survived to third instar, body size was substantially smaller than WT larvae (Fig. 3, A and B). It was previously reported that *Iswi* is important for chromosome condensation during mitosis, and *Iswi* LoF leads to mitotic recombination defects (41, 42). To investigate whether *Iswi* affects cell mitosis, we performed immunostaining with phosphorylated histone H3 (pH3), a proliferation marker for mitotic cells. We observed that in the brain lobes, the number of pH3⁺ positive cells was significantly decreased in *Iswi*² larvae (Fig. 3, C and D). We next asked whether *Iswi* may play a role in neuronal development. To accomplish this, we used *Drosophila* dendritic arborization (da) sensory neurons, which provide a suitable system to study neuronal development and dendritic morphology. There are four classes of da neurons, with class IV da (C4da) neurons extending the most complex and highly branched dendrites (43). We found that in *Iswi*², the dendrite complexity of C4da neurons was decreased. Both the total dendrite length and dendritic branch number exhibited a significant reduction (fig. S2, B to D), indicating that *Iswi* is important for dendrite morphogenesis. Furthermore, *Iswi* LoF also caused a tiling defect between C4da neurons *ddaC* and *v'ada*. Tiling refers to a phenomenon in which the dendrites of adjacent neurons establish complete but nonredundant interaction to occupy the space between the cell bodies as observed in WT larvae (44). In *Iswi*² larvae, however, the space is not fully covered because there is a significantly enlarged gap in the dendritic field between *ddaC* and *v'ada* (Fig. 3, E and F). These results suggest that *Iswi* plays a pleiotropic role during fly larval development, highlighting its involvement in neural proliferation and morphogenesis.

We next expressed *Iswi* RNAi under the control of *elav-Gal4*, a pan-neuronal driver (45), to determine whether *Iswi* is cell-autonomously required in neurons. Neural-specific knockdown of *Iswi* leads to significantly smaller brain size in adult flies (Fig. 4, A and B). Moreover, in the *Iswi* knockdown brains, we observed severe structural deficits of the mushroom body, the learning and memory center of the fly (46). Compared to control, the volume of both the vertical lobe and the horizontal lobe is markedly reduced after *Iswi* knockdown, with bilaterally missing vertical lobe and reduction of the horizontal lobe (Fig. 4, C to E). Consistent with these findings, Gong *et al.* (47) reported that *Iswi* knockdown in flies results in mushroom body morphologic abnormalities, as well as disrupted sleep, circadian rhythmicity, memory, and social behaviors, suggesting that *Iswi* is required during development for numerous adult behaviors.

As motor delay was reported in several patients, we next examined the locomotor function in *Iswi* knockdown flies by the negative geotaxis assay (a climbing test). We found that while ~80% of control flies climbed to or past the target distance, only a small portion of *Iswi* knockdown flies (less than 20%) showed normal climbing ability (Fig. 4F), indicating that neural knockdown of *Iswi* severely impaired the motor skills in flies. Together, these data indicate that *Iswi* is necessary for brain development and function in flies.

SMARCA5 WT but not mutants rescue the defects observed after *Iswi* LoF

To determine the functional consequences of the SMARCA5 variants identified in individuals 1 and 2, we generated transgenic flies with inducible expression of WT SMARCA5 (SMARCA5^{WT}), SMARCA5^{R592Q} and SMARCA5^{268-319del}, respectively. We found that these variants did not change SMARCA5's localization in the nucleus (fig. S2A). We investigated whether human SMARCA5^{WT} and variants could rescue the defects observed in *Iswi*² larvae and neural-specific *Iswi* knockdown flies. First, we expressed SMARCA5^{WT} and the two human variants in *Iswi*² larvae under the control of *Act5C-Gal4*, which drives the expression ubiquitously (48), and found that SMARCA5^{WT} expression was sufficient to rescue the larval body size similar to WT. In contrast, SMARCA5^{R592Q} and SMARCA5^{268-319del} only partially rescued the body length in *Iswi*² larvae (Fig. 3, A and B). Second, we examined whether the expression of WT or mutant SMARCA5 rescued the decreased cellular proliferation observed in *Iswi*² larval brain lobes. When using the *elav-Gal4* driver to express SMARCA5^{WT} in *Iswi* LoF larvae, we found that SMARCA5^{WT} robustly rescued the proliferation deficits, while no rescue was observed when expressing the two patient variants.

Third, we expressed SMARCA5^{WT} in C4da neurons of *Iswi*² larvae using the C4da neuron-specific *ppk-Gal4* driver (43) and found that SMARCA5^{WT} substantially rescued the tiling deficit between *ddaC* and *v'ada*, resulting in significantly decreased gap area in the dendritic field. Perhaps because *Drosophila* *Iswi* is the ortholog of the human *SMARCA1* and *SMARCA5*, expressing SMARCA5 only partially restored the neurodevelopmental defects in *Iswi*² (Fig. 3, E and F). Notably, both human SMARCA5 variants completely failed to rescue the tiling phenotype in *Iswi*² (Fig. 3, E and F). Overexpressing SMARCA5^{WT} in WT larvae reduced dendritic complexity (fig. S2, B to D), similar to the phenotype observed in *Iswi*², suggesting that the precise control of *Iswi* expression is crucial for normal dendrite morphogenesis. While the expression of SMARCA5^{R592Q} also caused impaired dendrite outgrowth and branching, the dendrite length and branch number in SMARCA5^{268-319del}-overexpressing

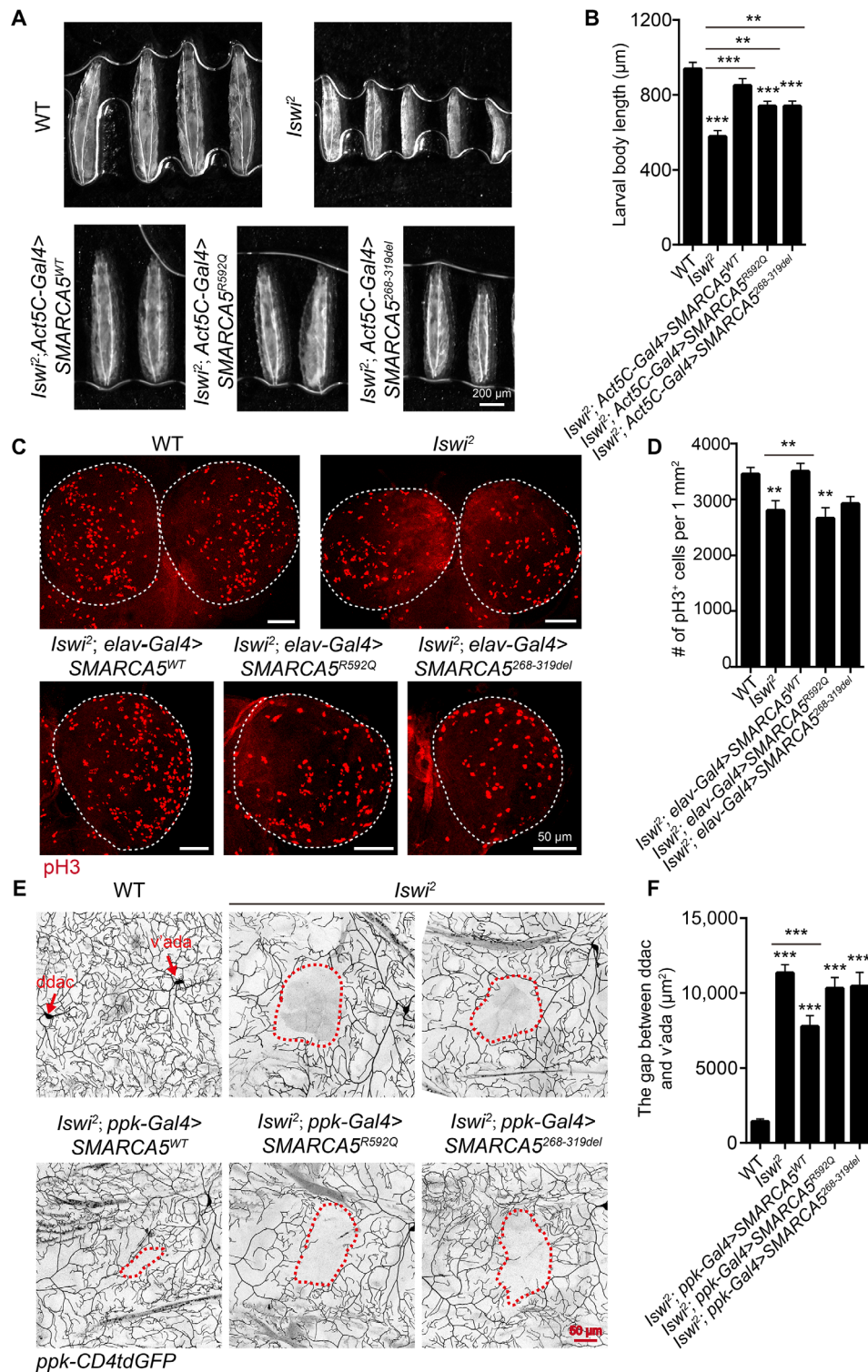


Fig. 3. *Iswi* LoF leads to developmental defects in *Drosophila* larvae. (A and B) Compared with WT, larval body size is significantly smaller in *Iswi²* third-instar larvae, which can be rescued by the expression of SMARCA5^{WT} by *Act5C-Gal4*. (A) Images showing larvae of different genotypes. Scale bar, 200 µm. (B) Quantification of larval body length. *N* = 30 to 41 larvae. (C and D) In the brain lobes of *Iswi²* larvae, the number of pH3⁺ positive mitotic cells is significantly decreased. *N* = 12 to 17 brain lobes. Expressing SMARCA5^{WT} by *elav>Gal4* is sufficient to rescue the decreased proliferation in *Iswi* LoF larvae. (C) The brains were dissected from third-instar larvae and stained with pH3. Scale bar, 50 µm. (D) Quantification of pH3⁺ positive mitotic cells; *P* = 0.0090. (E and F) In *Iswi²*, C4da ddaC and vada neurons exhibit dendritic tiling defects. SMARCA5^{WT}, but not patient variants, partially rescues the tiling defects. Scale bar, 50 µm. (E) The red dashed circles outline the gap area between C4da ddaC and vada neurons. (F) Quantification of the gap in C4da neuron dendritic field; *N* = 17 to 34 dendritic fields from 4 to 5 larvae. All data are means ± SEM. The data were analyzed by one-way analysis of variance (ANOVA) followed by Dunnett’s multiple comparisons test; ***P* < 0.01, ****P* < 0.001.

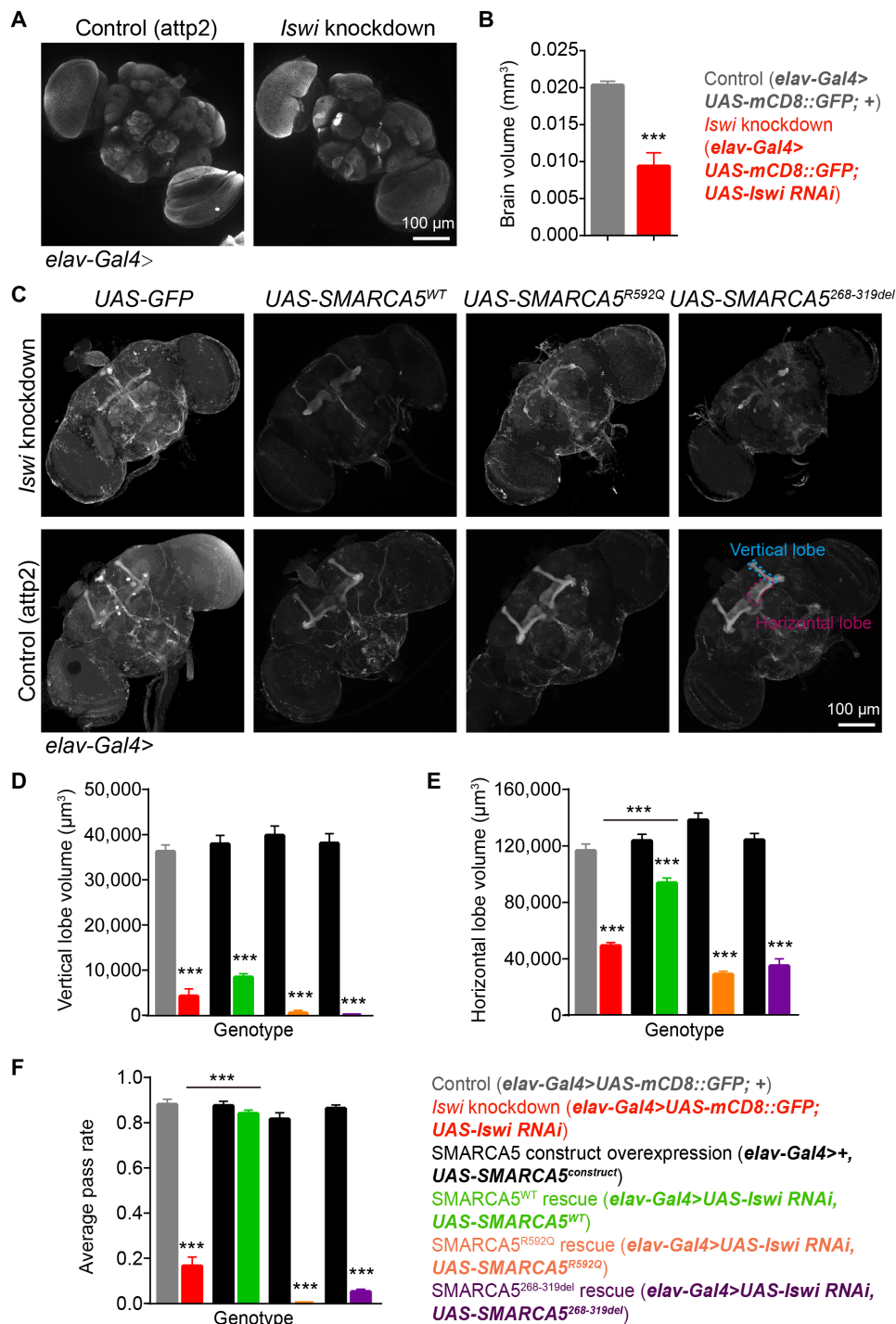


Fig. 4. *Iswi* neural-specific knockdown causes abnormal brain structure and motor deficits in adult flies. (A and B) *Iswi* neural-specific knockdown leads to smaller brain size compared with control flies. (A) Representative images of fly brains of control and *Iswi* knockdown flies. Scale bar, 100 µm. (B) Quantification of adult fly brain volume. $N = 6$, $P = 0.0002$. (C to E) *Iswi* neural-specific knockdown affects mushroom body structure in adult flies. While expressing *SMARCA5^{WT}* partially rescues the structure, the patient variants are not able to rescue mushroom body morphology. Cyan and magenta dashed lines outline the vertical lobe and horizontal lobe of the mushroom body in the right hemisphere, respectively. $N = 11$ to 35 brains. (C) Representative images of fly brains from different groups. Mushroom bodies are marked by FasII staining. Scale bar, 100 µm. (D) Quantification of vertical lobe volume. (E) Quantification of horizontal lobe volume. *SMARCA5^{WT}* rescue significantly increases the horizontal lobe volume in *Iswi* knockdown flies. (F) The negative geotaxis test shows that *Iswi* knockdown leads to locomotion deficit in flies. Expression of *SMARCA5^{WT}* in *Iswi* knockdown flies is able to rescue the climbing deficit to control levels, while *SMARCA5^{R592Q}* and *SMARCA5^{268-319del}* mutants fail to rescue. $N = 3$ to 12 groups, with each group containing 10 flies. All data are means \pm SEM. The data were analyzed by unpaired *t* test or one-way ANOVA followed by Tukey's multiple comparison test; $***P < 0.001$.

neurons were comparable to WT flies without transgenic expression of human SMARCA5 (fig. S2, B to D). We did not observe dendritic tiling defects in any of the three overexpression transgenic lines. These results suggest that although both variants jeopardized normal function of SMARCA5, they appear to differ in their mutagenic strength and may not be complete LoF.

Last, human WT SMARCA5 partially reversed the mushroom body morphologic abnormalities and fully rescued locomotion defects induced by neural-specific *Iswi* knockdown. We found that the expression of SMARCA5^{WT} partially restored horizontal lobe volume of the mushroom body, although it had little effect on the vertical lobes (Fig. 4, C to E). Comparatively, expressing either SMARCA5^{R592Q} or SMARCA5^{268-319del} was unable to rescue the morphological defects. In the negative geotaxis test, SMARCA5^{WT} fully rescued the climbing deficit in *Iswi* knockdown flies, resulting in similar motor performance as control flies, while the patient variants failed to improve climbing capacity (Fig. 4F).

DISCUSSION

We describe a novel syndromic neurodevelopmental disorder caused by de novo or dominantly inherited variants in *SMARCA5*, a gene that encodes an ATPase motor protein in the ISWI chromatin remodeler complex and that is extremely intolerant to both LoF (pLI = 1) and missense ($Z = 5.42$) variants based on the gnomAD population database. We identified seven missense variants, one splice-altering variant that led to exon skipping and in-frame deletion, and one recurrent in-frame deletion in 12 individuals from 10 unrelated families from around the world. The individuals in our study demonstrated a broad range of clinical features, as is not uncommon in neurodevelopmental disorders associated with pathogenic variants in aforementioned chromatin remodeling complexes (i.e., SWI/SNF, CHD, and ISWI) that vary from isolated autism to syndromic intellectual disability (5, 17, 49, 50). The most consistent clinical findings in our cohort are postnatal microcephaly and short stature observed in 10 of 12 individuals as well as developmental delay in 8 of 10 individuals, although, again, the severity of these delays varies widely from mild to severe (individual 7). Individual 10 has macrocephaly with a variant outside the helicase C-terminal domain, and individual 11 is normocephalic with a variant in HSS domains; both of these individuals have delays in motor and speech development but have normal stature, illustrating phenotypic variability. Conversely, individuals 1 and 8 have postnatal microcephaly and short stature but normal development with variants in the helicase ATP-binding domain. Varying degrees of developmental delay have been consistently reported in neurodevelopmental disorders associated with pathogenic variants involved in chromatin remodeling complexes. Similarly, varying head size ranging from microcephalic to macrocephalic is also frequently observed, for example, in *SMARCB1* and *CHD3* (50, 51). It is widely acknowledged that different variants within different functional domains of a gene can cause different phenotypes. Although the numbers are relatively small, when comparing phenotypes to identified variants, no clear genotype-phenotype correlation was established in this cohort. It is noteworthy that variants in *SMARCA1*, which is highly homologous to *SMARCA5*, have been associated with distinct phenotypes such as Rett syndrome, Coffin-Siris-like syndrome, and sporadic schizophrenia (19, 20, 52). This can be explained by different temporal and spatial expression patterns of both genes, although *SMARCA1*

and *SMARCA5* could be interchangeably present in the different ISWI complexes that often have overlapping and complex-specific functions.

SMARCA5 is located at 4q31.21, a region overlapping with the deletions observed in the 4q deletion syndrome, which is characterized by a broad clinical spectrum and phenotypic variability (53). Review of the literature revealed that two subjects have interstitial deletions encompassing the *SMARCA5* gene. One patient with 14-Mb deletion (4q28.3-31.23) has development delay, growth failure, ventricular septum defect, and craniofacial dysmorphisms (54), whereas the other subject with a 6-Mb deletion has only mild speech delay (55). Searching the Decipher database returned 14 participants that have deletions containing *SMARCA5* with a range of heterogeneity in clinical findings. Because all of these deletions are larger than 6-Mb and include many other genes, it is unclear how haploinsufficiency of *SMARCA5* contributes to their specific phenotypes, but it suggests that heterozygous *SMARCA5* deletion is compatible with life. On the basis of our findings, we propose that *SMARCA5* should be considered in the context of 4q deletion syndrome.

In general, this novel *SMARCA5*-associated syndrome reported here appears to result in a less severe phenotype when compared to other neurodevelopmental disorders due to pathogenic variants in *ARID*, *SMARC*, and *CHD* gene families, where almost all of the variants occur de novo and parent-child transmission is rarely documented (50, 56). We present here a three-generation pedigree (for individuals 4 to 6) segregating a deleterious missense variant. It is interesting to note that individual 4's maternal grandfather also has short stature (indicated in the pedigree; fig. S3); however, he has a pathogenic variant in *TLK2* [NM_006852.3:c.364C>T, p.(Arg122*)] that is associated with "Mental retardation, autosomal dominant 57" (OMIM no. 618050), which also includes short stature. This variant is not inherited by individuals 5 and 6, as confirmed by exome sequencing. Although *SMARCA5*-associated neurological complications are generally mild, postnatal proportionate short stature and microcephaly are rather predominant, with SDs ranging from -2 to -4.78 for height, and -2 to -6.21 for head circumference, in 8 of 10 probands. It has been widely appreciated that many rare diseases of the epigenetic machinery demonstrate significant phenotype overlap. Individuals presented here have craniofacial dysmorphisms, and some facial features overlap with *SMARCA2*-associated blepharophimosis intellectual disability syndrome (57), including blepharophimosis, short palpebral fissures, epicanthal folds, high arched and sparse eyebrows, and short metacarpals. Recently, pathogenic variants of *BPTF*, encoding a noncatalytic subunit of ISWI complex, have been implicated in a neurodevelopmental disorder (18). Phenotype comparison of *BPTF*- and *SMARCA5*-associated disorders reveals additional similarities, including developmental delay, intellectual disability, motor delay, speech delay, failure to thrive, dysmorphisms, and limb abnormalities. Overall, individuals with the *SMARCA5*-associated phenotypes appear to share similar dysmorphic features and clinical histories, including blepharophimosis, short palpebral fissures, periorbital fullness, wide/high nasal bridge, a thin or tented upper lip, short/smooth philtrum, high arched, sparse, or broad eyebrows, and hallux valgus, but each of the shared clinical findings is relatively nonspecific. Additional individuals and further assessment will be required to further clarify the clinical spectrum and constellation of features associated with this novel disorder to subsequently assist in the clinical diagnosis; however, *SMARCA5* gene sequencing should be

considered in patients with failure to thrive, short stature, microcephaly, and dysmorphic features.

Our phenotypic analyses in the fly *Iswi* LoF models and human patients emphasize the pleiotropic and critical role of SMARCA5 and the SNF2H-containing chromatin remodeling complexes in nervous system development. We observed that LoF mutants of its *Drosophila* ortholog *Iswi* led to decreased larval body size and sensory dendrite complexity, together with a tiling defect. Such dendritic defects have also been described in cerebellar Purkinje neurons in conditional knockout of *Snf2h* in mice (34). In addition, analyses of pan-neuronal knockout and telencephalon-specific knockout of *Snf2h* in mice have both revealed a smaller brain phenotype (34, 58). Apart from its previously reported function in cell proliferation/stem cell self-renewal (59) and hence smaller head/microcephaly, we identified its requirement in postmitotic neurons. Specifically, we found that *Iswi* LoF leads to defects in sensory neuron dendrite tiling and mushroom body development, highlighting its underappreciated role in neural circuit assembly (47). This likely contributes to the behavioral deficits such as impaired locomotion in the *Iswi* knockdown flies and intellectual disability, hypotonia, and speech delay in patients. Nevertheless, the patient variants, SMARCA5^{R592Q} and SMARCA5^{268-319del}, largely failed to replace *Iswi* in flies, highlighting the functional effect of the variants that we identified. Given that both variants could partially rescue the reduced body size in *Iswi*², and that the overexpression of SMARCA5^{R592Q} in neurons affects their dendrite morphology, these two variants may not be complete LoF alleles and may retain partial function, allowing it to interact with the dendrite morphogenesis machinery. Modeling variants in the three-dimensional structure suggests that they may disrupt interactions of SMARCA5 with the nucleosome and, in turn, affect ATPase binding. An emerging question is how SMARCA5 and, more generally, the chromatin remodelers exert their diverse functions under various developmental scenarios. Therefore, an imminent task is to identify the DNA substrates processed by the remodelers at a particular time point and in a specialized tissue niche, which could be potential therapeutic targets. Together, our functional studies of the SMARCA5 missense variants suggest that they are hypomorphic alleles, although a dominant effect mechanism through competitive inhibition of the WT functional allele in the ISWI complex is also possible.

In summary, we identify and phenotypically characterize a novel neurodevelopmental syndrome that overlaps with conditions caused by variants in different subunits of chromatin remodeling complexes. Frequent features include postnatal short stature and microcephaly, in addition to shared dysmorphia. Our findings in a fly in vivo model highlight the important and previously underappreciated role of the ISWI family proteins in dendrite morphogenesis, neural circuit formation, and diverse behaviors. In conclusion, this study expands the spectrum of ISWI-related disorders and extends the tally of causative genes in neurodevelopmental disorders.

METHODS AND MATERIALS

Research participants

Informed consent was obtained from all the families according to protocols approved by local institutional review boards and human research ethics committees. Permission for clinical photographs was given separately. Individual 2 was recruited to the Murdoch Children's Research Institute's Undiagnosed Diseases Project Victoria for gene

discovery after a nondiagnostic clinical exome. Trio exome sequencing was undertaken at the Broad Center for Mendelian Genomics.

Genetic analysis

Genomic DNA was extracted from whole blood from the affected children and their parents. Exome sequencing was performed with a variety of standard capture kits, and data analysis was performed independently. In patients 9 and 11, exome sequencing was performed in the framework of the German project "TRANSLATE NAMSE," an initiative from the National Action League for People with Rare Diseases [Nationales Aktionsbündnis für Menschen mit Seltenen Erkrankungen (NAMSE)] facilitating innovative genetic diagnostics for individuals with suggested rare diseases. RNA was extracted from fibroblasts, and an LCL was obtained from individual 1 and control LCLs using the RNeasy Mini Kit with on-column DNaseI digestion (Qiagen, catalog nos. 74104 and 79254), according to the manufacturer's instructions. Total RNA (2 µg) was reverse-transcribed to cDNA with the High Capacity cDNA Reverse Transcription Kit (Thermo Fisher Scientific, catalog no. 4368814) using random primers. PCR was performed with the cDNA as template using primers 5'-TTGCACTCGATTTGAAGACTCT-3' and 5'-AGTTAAGAAGT-GACCACAGCTC-3'. cDNA from a commercial pooled tissue cDNA library (qPCR Human Reference cDNA, random primed; Clontech, catalog no. 639654) was included as a control. Subsequent Sanger sequencing was performed using the same primers.

Fly stocks

Ppk-CD4tdGFP, *ppk-Gal4*, *UAS-Iswi RNAi*, *elav-Gal4*, *UAS-mCD8::GFP*, and *P{CaryP}attP2* have been previously described (47, 60). To generate the *UAS-SMARCA5^{WT}*, *UAS-SMARCA5^{R592Q}*, and *UAS-SMARCA5^{268-319del}* stocks, the coding sequences were cloned into a pACU2 vector, and the constructs were then injected (Rainbow Transgenic Flies Inc). The experimental procedures have been approved by the Institutional Biosafety Committee at the Children's Hospital of Philadelphia.

Live imaging in flies

Live imaging was performed as described (61). In brief, embryos were collected for 2 to 24 hours on yeast grape juice agar plates and were aged at 25°C. At 96 hours after egg laying, larvae were mounted in 90% glycerol under coverslips sealed with grease and imaged using a Zeiss LSM 880 microscope. Neurons were reconstructed with Neurostudio for dendrite morphology analyses.

Immunohistochemistry

Third-instar larvae were dissected, and tissues were subjected to immunostaining as described according to standard protocols. The following antibodies were used: mouse anti-FLAG antibody (F3156, 1:1000, Sigma-Aldrich), rat anti-histone H3 (phospho-S28) antibody (ab10543, Abcam, 1:500), and fluorescence-conjugated secondary antibodies (1:1000, Jackson ImmunoResearch).

Negative geotaxis test

Negative geotaxis was performed as described previously (62). Three days after eclosion, 10 flies of the same genotype were placed in a 20-cm-high vial. After 2-min adaptation, the vial was gently tapped against the table so the flies would be knocked to the bottom of the vial. The pass rate is defined as the percentage of flies climbing beyond the 8-cm mark within 10 s. Each vial was assayed 10 times,

and the average pass rate is defined as the average across 10 trials. Male and female flies were picked randomly.

SUPPLEMENTARY MATERIALS

Supplementary material for this article is available at <http://advances.sciencemag.org/cgi/content/full/7/20/eabf2066/DC1>

[View/request a protocol for this paper from Bio-protocol.](#)

REFERENCES AND NOTES

- C. R. Clapier, B. R. Cairns, The biology of chromatin remodeling complexes. *Annu. Rev. Biochem.* **78**, 273–304 (2009).
- G. W. E. Santen, E. Aten, Y. Sun, R. Almomani, C. Gilissen, M. Nielsen, S. G. Kant, I. N. Snoeck, E. A. J. Peeters, Y. Hillhorst-Hofstee, M. W. Wessels, N. S. den Hollander, C. A. L. Ruivenkamp, G.-J. B. van Ommen, M. H. Breuning, J. T. den Dunnen, A. van Haeringen, M. Kriek, Mutations in SWI/SNF chromatin remodeling complex gene *ARID1B* cause Coffin-Siris syndrome. *Nat. Genet.* **44**, 379–380 (2012).
- K. C. J. Nixon, J. Rousseau, M. H. Stone, M. Sarikahya, S. Ehresmann, S. Mizuno, N. Matsumoto, N. Miyake, D. D. D. Study, D. Baralle, S. McKee, K. Izumi, A. L. Ritter, S. Heide, D. Heron, C. Depienne, H. Titheradge, J. M. Kramer, P. M. Campeau, A syndromic neurodevelopmental disorder caused by mutations in *SMARCD1*, a core SWI/SNF subunit needed for context-dependent neuronal gene regulation in flies. *Am. J. Hum. Genet.* **104**, 596–610 (2019).
- Y. Tsurusaki, N. Okamoto, H. Ohashi, T. Koshi, Y. Imai, Y. Hibi-Ko, T. Kaname, K. Naritomi, H. Kawame, K. Wakui, Y. Fukushima, T. Homma, M. Kato, Y. Hiraki, T. Yamagata, S. Yano, S. Mizuno, S. Sakazume, T. Ishii, T. Nagai, M. Shiina, K. Ogata, T. Ohta, N. Niikawa, S. Miyatake, I. Okada, T. Mizuguchi, H. Doi, H. Saitou, N. Miyake, N. Matsumoto, Mutations affecting components of the SWI/SNF complex cause Coffin-Siris syndrome. *Nat. Genet.* **44**, 376–378 (2012).
- K. Machol, J. Rousseau, S. Ehresmann, T. Garcia, T. T. M. Nguyen, R. C. Spillmann, J. A. Sullivan, V. Shashi, Y.-h. Jiang, N. Stong, E. Fiala, M. Willing, R. Pfundt, T. Kleefstra, M. T. Cho, H. M. Laughlin, M. R. Piera, C. Orellana, F. Martinez, A. Caro-Llopis, S. Monfort, T. Roscioli, C. Y. Nixon, M. F. Buckley, A. Turner, W. D. Jones, P. M. van Hasselt, F. C. Hofstede, K. L. I. van Gassen, A. S. Brooks, M. A. van Slegtenhorst, K. Lachlan, J. Sebastian, S. Madan-Khetarpal, D. Sonal, N. Sakkubai, J. Thevenon, L. Faivre, A. Maurel, S. Petrovski, I. D. Krantz, J. M. Tarpinian, J. A. Rosenfeld, B. H. Lee; Undiagnosed Diseases Network, P. M. Campeau, Expanding the spectrum of BAF-related disorders: De novo variants in *SMARCC2* cause a syndrome with intellectual disability and developmental delay. *Am. J. Hum. Genet.* **104**, 164–178 (2019).
- D. Wiczorek, N. Bögershausen, F. Beleggia, S. Steiner-Haldenstädt, E. Pohl, Y. Li, E. Milz, M. Martin, H. Thiele, J. Altmüller, Y. Alanay, H. Kayserili, L. Klein-Hitpass, S. Böhringer, A. Wollstein, B. Albrecht, K. Boduroglu, A. Caliebe, K. Chrzanosowska, O. Cogulu, F. Cristofoli, J. C. Czeschik, K. Devriendt, M. T. Dotti, N. Elcioglu, B. Gener, T. O. Goecke, M. Krajewska-Walasek, E. Guillén-Navarro, J. Hayek, G. Houge, E. Kilic, P. Ö. Simsek-Kiper, V. López-González, A. Kuechler, S. Lyonnet, F. Mari, A. Marozza, M. M. Dramard, B. Mikat, G. Morin, F. Morice-Picard, F. Özkinay, A. Rauch, A. Renieri, S. Tinschert, G. E. Utine, C. Vilain, R. Vivarelli, C. Zweier, P. Nürnberg, S. Rahmann, J. Vermeesch, H.-J. Lüdecke, M. Zeschnick, B. Wollnik, A comprehensive molecular study on Coffin-Siris and Nicolaides-Baraitser syndromes identifies a broad molecular and clinical spectrum converging on altered chromatin remodeling. *Hum. Mol. Genet.* **22**, 5121–5135 (2013).
- L. Shang, M. T. Cho, K. Retterer, L. Folk, J. Humberson, L. Rohena, A. Sidhu, S. Saliganan, A. Iglesias, P. Vitazka, J. Juusola, A. H. O'Donnell-Luria, Y. Shen, W. K. Chung, Mutations in *ARID2* are associated with intellectual disabilities. *Neurogenetics* **16**, 307–314 (2015).
- G. Vasileiou, S. Vergarajauregui, S. Endeley, B. Popp, C. Büttner, A. B. Ekici, M. Gerard, N. C. Bramswig, B. Albrecht, J. Clayton-Smith, J. Morton, S. Tomkins, K. Low, A. Weber, M. Wenzel, J. Altmüller, Y. Li, B. Wollnik, G. Hoganson, M.-R. Plona, M. T. Cho; Deciphering Developmental Disorders Study, C. T. Thiel, H.-J. Lüdecke, T. M. Strom, E. Calpena, A. O. M. Wilkie, D. Wiczorek, F. B. Engel, A. Reis, Mutations in the BAF-complex subunit *DPF2* are associated with Coffin-Siris syndrome. *Am. J. Hum. Genet.* **102**, 468–479 (2018).
- J. K. J. Van Houdt, B. A. Nowakowska, S. B. Sousa, B. D. C. van Schaik, E. Seuntjens, N. Avonce, A. Sifrim, O. A. Abdul-Rahman, M.-J. H. van den Boogaard, A. Bottani, M. Castori, V. Cormier-Daire, M. A. Deardorff, I. Filges, A. Fryer, J.-P. Fryns, S. Gana, L. Garavelli, G. Gillissen-Kaesbach, B. D. Hall, D. Horn, D. Huylebroeck, J. Klapecki, M. Krajewska-Walasek, A. Kuechler, M. A. Lines, S. Maas, K. D. MacDermot, S. M. Kee, A. Magee, S. A. de Man, Y. Moreau, F. Morice-Picard, E. Obersztyn, J. Pilch, E. Rosser, N. Shannon, I. Stolte-Dijkstra, F. B. Engel, C. Vilain, A. Vogels, E. Wakeling, D. Wiczorek, L. Wilson, O. Zuffardi, A. H. C. van Kampen, K. Devriendt, R. Hennekam, J. R. Vermeesch, Heterozygous missense mutations in *SMARCA2* cause Nicolaides-Baraitser syndrome. *Nat. Genet.* **44**, 445–449 (2012).
- D. Wolff, S. Endeley, S. Azzarello-Burri, J. Hoyer, M. Zweier, I. Schanze, B. Schmitt, A. Rauch, A. Reis, C. Zweier, In-frame deletion and missense mutations of the C-terminal helicase domain of *SMARCA2* in three patients with Nicolaides-Baraitser syndrome. *Mol. Syndromol.* **2**, 237–244 (2012).
- C. Dias, S. B. Estruch, S. A. Graham, J. M. Rae, S. J. Sawiak, J. A. Hurst, S. K. Joss, S. E. Holder, J. E. V. Morton, C. Turner, J. Thevenon, K. Mellul, G. Sánchez-Andrade, X. Ibarra-Soria, P. Deriziotis, R. F. Santos, S.-C. Lee, L. Faivre, T. Kleefstra, P. Liu, M. E. Hurles; D. D. D. Study, S. E. Fisher, D. W. Logan, *BCL11A* haploinsufficiency causes an intellectual disability syndrome and dysregulates transcription. *Am. J. Hum. Genet.* **99**, 253–274 (2016).
- S. Bell, J. Rousseau, H. Peng, Z. Aouabed, P. Priam, J.-F. Theroux, M. Jefri, A. Tanti, H. Wu, I. Kolobova, H. Silveira, K. Manzano-Vargas, S. Ehresmann, F. F. Hamdan, N. Hettige, X. Zhang, L. Antonyan, C. Nassif, L. Ghaloul-Gonzalez, J. Sebastian, J. Vockley, A. G. Begtrup, I. M. Wentzensen, A. Crunk, R. D. Nicholls, K. C. Herman, J. L. Deignan, W. Al-Hertani, S. Efthymiou, V. Salpietro, N. Miyake, Y. Makita, M. Matsumoto, R. Østern, G. Houge, M. Hafström, E. Fassi, H. Houlden, J. S. Klein Wassink-Ruiter, D. Nelson, A. Goldstein, T. Dabir, J. van Gils, T. Bourgeron, R. Delorme, G. M. Cooper, J. E. Martinez, C. R. Finnilla, L. Carmant, A. Lortie, R. Oegema, K. van Gassen, S. G. Mehta, D. Huhle, R. A. Jamra, S. Martin, H. G. Brunner, D. Lindhout, M. Au, J. M. Graham Jr., C. Coubes, G. Turecki, S. Gravel, N. Mechawar, E. Rossignol, J. L. Michaud, J. Lessard, C. Ernst, P. M. Campeau, Mutations in *ACTL6B* cause neurodevelopmental deficits and epilepsy and lead to loss of dendrites in human neurons. *Am. J. Hum. Genet.* **104**, 815–834 (2019).
- J.-B. Rivière, B. W. M. van Bon, A. Hoischen, S. S. Kholmanskikh, B. J. O'Roak, C. Gilissen, S. Gijsen, C. T. Sullivan, S. L. Christian, O. A. Abdul-Rahman, J. F. Atkin, N. Chassaing, V. Drouin-Garraud, A. E. Fry, J.-P. Fryns, K. W. Gripp, M. Kempers, T. Kleefstra, G. M. S. Mancini, M. J. M. Nowaczyk, C. M. A. van Ravenswaaij-Arts, T. Roscioli, M. Marble, J. A. Rosenfeld, V. M. Siu, B. B. A. de Vries, J. Shendure, A. Verloes, J. A. Veltman, H. G. Brunner, M. E. Ross, D. T. Pilz, W. B. Dobyns, De novo mutations in the actin genes *ACTB* and *ACTG1* cause Baraitser-Winter syndrome. *Nat. Genet.* **44**, 440–444 (2012).
- A. Sifrim, M.-P. Hitz, A. Wilsdon, J. Breckpot, S. H. Al Turki, B. Thienpont, J. M. Rae, T. W. Fitzgerald, T. Singh, G. J. Swaminathan, E. Prigmore, D. Rajan, H. Abdul-Khalik, S. Banka, U. M. M. Bauer, J. Bentham, F. Berger, S. Bhattacharya, F. Bu'Lock, N. Canham, I.-G. Colgiu, C. Cosgrove, H. Cox, I. Daehner, A. Daly, J. Danesh, A. Fryer, M. Gewillig, E. Hobson, K. Hoff, T. Homfray; INTERVAL Study, A.-K. Kahlert, A. Ketley, H.-H. Kramer, K. Lachlan, A. K. Lampe, J. J. Louw, A. K. Manickar, D. Manase, K. P. McCarthy, K. Metcalfe, C. Moore, R. Newbury-Ecob, S. O. Omer, W. H. Ouweland, S.-M. Park, M. J. Parker, T. Pickard, M. O. Pollard, L. Robert, D. J. Roberts, J. Sambrook, K. Setchfield, B. Stiller, C. Thornborough, O. Toka, H. Watkins, D. Williams, M. Wright, S. Mital, P. E. F. Daubeny, B. Keavney, J. Goodship; UK10K Consortium, R. M. Abu-Sulaiman, S. Klaassen, C. F. Wright, H. V. Firth, J. C. Barrett, K. Devriendt, D. R. F. Patrick, J. D. Brook; Deciphering Developmental Disorders Study, M. E. Hurles, Distinct genetic architectures for syndromic and nonsyndromic congenital heart defects identified by exome sequencing. *Nat. Genet.* **48**, 1060–1065 (2016).
- K. Weiss, P. A. Terhal, L. Cohen, M. Bruccoleri, M. Irving, A. F. Martinez, J. A. Rosenfeld, K. Machol, Y. Yang, P. Liu, M. Walkiewicz, J. Beuten, N. Gomez-Ospina, K. Haude, C.-T. Fong, G. M. Enns, J. A. Bernstein, J. Fan, G. Gotway, M. Ghorbani; D. D. D. Study, K. van Gassen, G. R. Monroe, G. van Haften, L. Basel-Vanagaite, X.-J. Yang, P. M. Campeau, M. Muenke, De novo mutations in *CHD4*, an ATP-dependent chromatin remodeler gene, cause an intellectual disability syndrome with distinctive dysmorphisms. *Am. J. Hum. Genet.* **99**, 934–941 (2016).
- L. E. L. M. Vissers, C. M. A. van Ravenswaaij, R. Admiraal, J. A. Hurst, B. B. A. de Vries, I. M. Janssen, W. A. van der Vliet, E. H. L. P. G. Huys, P. J. de Jong, B. C. J. Hamel, E. F. P. M. Schoenmakers, H. G. Brunner, J. A. Veltman, A. G. van Kessel, Mutations in a new member of the chromodomain gene family cause CHARGE syndrome. *Nat. Genet.* **36**, 955–957 (2004).
- L. S. Blok, J. Rousseau, J. Twist, S. Ehresmann, M. Takaku, H. Venselaar, L. H. Rodan, C. B. Nowak, J. Douglas, K. J. Swoboda, M. A. Steeves, I. Sahai, C. T. R. M. Stumpel, A. P. A. Stegmann, P. Wheeler, M. Willing, E. Fiala, A. Kochhar, W. T. Gibson, A. S. A. Cohen, R. Agbahovbe, A. M. Innes, P. Y. B. Au, J. Rankin, I. J. Anderson, S. A. Skinner, R. J. Louie, H. E. Warren, A. Afenjar, B. Keren, C. Nava, J. Buratti, A. Isapof, D. Rodriguez, R. Lewandowski, J. Propst, T. van Essen, M. Choi, S. Lee, J. H. Chae, S. Price, R. E. Schnur, G. Douglas, I. M. Wentzensen, C. Zweier, A. Reis, M. G. Bialer, C. Moore, M. Koopmans, E. H. Brillstra, G. R. Monroe, K. L. I. van Gassen, E. van Binsbergen, R. Newbury-Ecob, L. Bownass, I. Bader, J. A. Mayr, S. B. Wortmann, K. J. Jakielski, E. A. Strand, K. Kloth, T. Bierhals, The DDD study, J. D. Roberts, R. H. Petrovich, S. Machida, H. Kurumizaka, S. Lelieveld, R. Pfundt, S. Jansen, P. Deriziotis, L. Faivre, J. Thevenon, M. Assoum, L. Shriberg, T. Kleefstra, H. G. Brunner, P. A. Wade, S. E. Fisher, P. M. Campeau, CHD3 helicase domain mutations cause a neurodevelopmental syndrome with macrocephaly and impaired speech and language. *Nat. Commun.* **9**, 4619 (2018).
- P. Stankiewicz, T. N. Khan, P. Szafranski, L. Slattery, H. Streff, F. Vetrini, J. A. Bernstein, C. W. Brown, J. A. Rosenfeld, S. Rednam, S. Scollon, K. L. Bergstrom, D. W. Parsons, S. E. Plon, M. W. Vieira, C. R. D. C. Quao, W. A. R. Barata, J. C. A. Guio, R. Armstrong, S. G. Mehta, P. Rump, R. Pfundt, R. Lewandowski, E. M. Fernandes, D. N. Shinde, S. Tang, J. Hoyer, C. Zweier, A. Reis, C. A. Bacino, R. Xiao, A. M. Breman, J. L. Smith; Deciphering

- Developmental Disorders Study, N. Katsanis, B. Bostwick, B. Popp, E. E. Davis, Y. Yang, Haploinsufficiency of the chromatin remodeler *BPTF* causes syndromic developmental and speech delay, postnatal microcephaly, and dysmorphic features. *Am. J. Hum. Genet.* **101**, 503–515 (2017).
19. E. Karaca, T. Harel, D. Pehlivan, S. N. Jhangiani, T. Gambin, Z. C. Akdemir, C. Gonzaga-Jauregui, S. Erdin, Y. Bayram, I. M. Campbell, J. O. V. Hunter, M. M. Atik, H. Van Esch, B. Yuan, W. Wiszniewski, S. Isikay, G. Yesil, O. O. Yuregir, S. T. Bozdogan, H. Aslan, H. Aydin, T. Tos, A. Aksoy, D. C. De Vivo, P. Jain, B. B. Geckinli, O. Sezer, D. Gul, B. Durmaz, O. Cogulu, F. Ozkinay, V. Topcu, S. Candan, A. H. Cebi, M. Ikbali, E. Y. Gulec, A. Gezdirci, E. Koparir, F. Ekici, S. Coskun, S. Cicek, K. Karaer, A. Koparir, M. B. Duz, E. Kirat, E. Fenercioglu, H. Ulucan, M. Seven, T. Guran, N. Elcioglu, M. S. Yildirim, D. Aktas, M. Alikasifoglu, M. Ture, T. Yakut, J. D. Overton, A. Yuksel, M. Ozen, D. M. Muzny, D. R. Adams, E. Boerwinkle, W. K. Chung, R. A. Gibbs, J. R. Lupski, Genes that affect brain structure and function identified by rare variant analyses of mendelian neurologic disease. *Neuron* **88**, 499–513 (2015).
 20. F. Lopes, M. Barbosa, A. Ameur, G. Soares, J. de Sá, A. I. Dias, G. Oliveira, P. Cabral, T. Temudo, E. Calado, I. F. Cruz, J. P. Vieira, R. Oliveira, S. Esteves, S. Sauer, I. Jonasson, A.-C. Syyvänen, U. Gyllensten, D. Pinto, P. Maciel, Identification of novel genetic causes of Rett syndrome-like phenotypes. *J. Med. Genet.* **53**, 190–199 (2016).
 21. T. Tsukiyama, C. Daniel, J. Tamkun, C. Wu, ISWI, a member of the SWI2/SNF2 ATPase family, encodes the 140 kDa subunit of the nucleosome remodeling factor. *Cell* **83**, 1021–1026 (1995).
 22. T. Ito, M. Bulger, M. J. Pazin, R. Kobayashi, J. T. Kadonaga, ACF, an ISWI-containing and ATP-utilizing chromatin assembly and remodeling factor. *Cell* **90**, 145–155 (1997).
 23. P. D. Varga-Weisz, M. Wilm, E. Bonte, K. Dumas, M. Mann, P. B. Becker, Chromatin-remodelling factor CHRAC contains the ATPases ISWI and topoisomerase II. *Nature* **388**, 598–602 (1997).
 24. G. LeRoy, G. Orphanides, W. S. Lane, D. Reinberg, Requirement of RSF and FACT for transcription of chromatin templates in vitro. *Science* **282**, 1900–1904 (1998).
 25. D. A. Bochar, J. Savard, W. Wang, D. W. Lafleur, P. Moore, J. Côté, R. Shiekhhattar, A family of chromatin remodeling factors related to Williams syndrome transcription factor. *Proc. Natl. Acad. Sci. U.S.A.* **97**, 1038–1043 (2000).
 26. O. Barak, M. A. Lazzaro, W. S. Lane, D. W. Speicher, D. J. Picketts, R. Shiekhhattar, Isolation of human NURF: A regulator of *Engrailed* gene expression. *EMBO J.* **22**, 6089–6100 (2003).
 27. R. A. Poot, G. Dellaire, B. B. Hulsmann, M. A. Grimaldi, D. F. Corona, P. B. Becker, W. A. Bickmore, P. D. Varga-Weisz, HuCHRAC, a human ISWI chromatin remodelling complex contains hACF1 and two novel histone-fold proteins. *EMBO J.* **19**, 3377–3387 (2000).
 28. G. S. Banting, O. Barak, T. M. Ames, A. C. Burnham, M. D. Kardel, N. S. Cooch, C. E. Davidson, R. Godbout, H. E. McDermaid, R. Shiekhhattar, CECR2, a protein involved in neurulation, forms a novel chromatin remodeling complex with SNF2L. *Hum. Mol. Genet.* **14**, 513–524 (2005).
 29. R. Strohner, A. Nemeth, P. Jansa, U. Hofmann-Rohrer, R. Santoro, G. Längst, I. Grummt, NoRC—A novel member of mammalian ISWI-containing chromatin remodeling machines. *EMBO J.* **20**, 4892–4900 (2001).
 30. M.-A. Hakimi, D. A. Bochar, J. A. Schmiesing, Y. Dong, O. G. Barak, D. W. Speicher, K. Yokomori, R. Shiekhhattar, A chromatin remodelling complex that loads cohesin onto human chromosomes. *Nature* **418**, 994–998 (2002).
 31. L. Bozhenok, P. A. Wade, P. Varga-Weisz, WSTF-ISWI chromatin remodeling complex targets heterochromatic replication foci. *EMBO J.* **21**, 2231–2241 (2002).
 32. M. Oppikofer, T. Bai, Y. Gan, B. Haley, P. Liu, W. Sandoval, C. Ciferri, A. G. Cochran, Expansion of the ISWI chromatin remodeler family with new active complexes. *EMBO Rep.* **18**, 1697–1706 (2017).
 33. A. Aguirre, N. Montserrat, S. Zacchigna, E. Nivet, T. Hishida, M. N. Krause, L. Kurian, A. Ocampo, E. Vazquez-Ferrer, C. Rodriguez-Esteban, S. Kumar, J. J. Moresco, J. R. Yates III, J. M. Campistol, I. Sancho-Martinez, M. Giacca, J. C. Izpisua Belmonte, In vivo activation of a conserved microRNA program induces mammalian heart regeneration. *Cell Stem Cell* **15**, 589–604 (2014).
 34. M. Alvarez-Saavedra, Y. De Repentigny, P. S. Lagali, E. V. Raghu Ram, K. Yan, E. Hashem, D. Ivanochko, M. S. Huh, D. Yang, A. J. Mears, M. A. Todd, C. P. Corcoran, E. A. Bassett, N. J. Tokarew, J. Kokavec, R. Majumder, I. Ioshikhes, V. A. Wallace, R. Kothary, E. Meshorer, T. Stopka, A. I. Skoultschi, D. J. Picketts, Snf2h-mediated chromatin organization and histone H1 dynamics govern cerebellar morphogenesis and neural maturation. *Nat. Commun.* **5**, 4181 (2014).
 35. M. A. Lazzaro, D. J. Picketts, Cloning and characterization of the murine *Imitation Switch* (ISWI) genes: Differential expression patterns suggest distinct developmental roles for Snf2h and Snf2l. *J. Neurochem.* **77**, 1145–1156 (2001).
 36. N. Sobreira, F. Schiettecatte, D. Valle, A. Hamosh, GeneMatcher: A matching tool for connecting investigators with an interest in the same gene. *Hum. Mutat.* **36**, 928–930 (2015).
 37. J. P. Armache, N. Gamarra, S. L. Johnson, J. D. Leonard, S. Wu, G. J. Narlikar, Y. Cheng, Cryo-EM structures of remodeler-nucleosome intermediates suggest allosteric control through the nucleosome. *eLife* **8**, e46057 (2019).
 38. J. A. Goldman, J. D. Garlick, R. E. Kingston, Chromatin remodeling by imitation switch (ISWI) class ATP-dependent remodelers is stimulated by histone variant H2A.Z. *J. Biol. Chem.* **285**, 4645–4651 (2010).
 39. H. T. Dao, B. E. Dul, G. P. Dann, G. P. Liszczak, T. W. Muir, A basic motif anchoring ISWI to nucleosome acidic patch regulates nucleosome spacing. *Nat. Chem. Biol.* **16**, 134–142 (2020).
 40. T. Grüne, J. Brzeski, A. Eberharter, C. R. Clapier, D. F. V. Corona, P. B. Becker, C. W. Müller, Crystal structure and functional analysis of a nucleosome recognition module of the remodeling factor ISWI. *Mol. Cell* **12**, 449–460 (2003).
 41. R. Deuring, L. Fanti, J. A. Armstrong, M. Sarte, O. Papoulas, M. Prestel, G. Daubresse, M. Verardo, S. L. Moseley, M. Berloco, T. Tsukiyama, C. Wu, S. Pimpinelli, J. W. Tamkun, The ISWI chromatin-remodeling protein is required for gene expression and the maintenance of higher order chromatin structure in vivo. *Mol. Cell* **5**, 355–365 (2000).
 42. D. F. V. Corona, G. Siriaco, J. A. Armstrong, N. Snarskaya, S. A. McClymont, M. P. Scott, J. W. Tamkun, ISWI regulates higher-order chromatin structure and histone H1 assembly in vivo. *PLoS Biol.* **5**, e232 (2007).
 43. W. B. Grueber, B. Ye, C.-H. Yang, S. Younger, K. Borden, L. Y. Jan, Y.-N. Jan, Projections of *Drosophila* multidendritic neurons in the central nervous system: Links with peripheral dendrite morphology. *Development* **134**, 55–64 (2007).
 44. W. B. Grueber, L. Y. Jan, Y. N. Jan, Tiling of the *Drosophila* epidermis by multidendritic sensory neurons. *Development* **129**, 2867–2878 (2002).
 45. L. Luo, Y. J. Liao, L. Y. Jan, Y. N. Jan, Distinct morphogenetic functions of similar small GTPases: *Drosophila* Drac1 is involved in axonal outgrowth and myoblast fusion. *Genes Dev.* **8**, 1787–1802 (1994).
 46. Y. Aso, D. Hattori, Y. Yu, R. M. Johnston, N. A. Iyer, T.-T. Ngo, H. Dionne, L. F. Abbott, R. Axel, H. Tanimoto, G. M. Rubin, The neuronal architecture of the mushroom body provides a logic for associative learning. *eLife* **3**, e04577 (2014).
 47. N. N. Gong, L. C. Dilley, C. E. Williams, E. H. Moscato, M. Szuperak, Q. Wang, M. Jensen, S. Girirajan, T. Y. Tan, M. A. Deardorff, D. Li, Y. Song, M. S. Kayser, The chromatin remodeler ISWI acts during *Drosophila* development to regulate adult sleep. *Sci. Adv.* **7**, eabe2597 (2021).
 48. K. Ito, W. Awano, K. Suzuki, Y. Hiromi, D. Yamamoto, The *Drosophila* mushroom body is a quadruple structure of clonal units each of which contains a virtually identical set of neurons and glial cells. *Development* **124**, 761–771 (1997).
 49. N. Bögershausen, B. Wollnik, Mutational landscapes and phenotypic spectrum of SWI/SNF-related intellectual disability disorders. *Front. Mol. Neurosci.* **11**, 252 (2018).
 50. T. G. Drivas, D. Li, D. Nair, J. T. Alaimo, M. Alders, J. Altmüller, T. S. Barakat, E. M. Bebin, N. L. Bertsch, P. R. Blackburn, A. Blesson, A. M. Bouman, K. Brockmann, P. Brunelle, M. Burmeister, G. M. Cooper, J. Denecke, A. Dieux-Coëslier, H. Dubbs, A. Ferrer, D. Gal, L. E. Bartik, L. B. Gunderson, L. Hasadsri, M. Jain, C. Karimov, B. Keena, E. W. Klee, K. Kloth, B. Lace, M. Macchiariolo, J. L. Marcadier, J. M. Milunsky, M. P. Napier, X. R. Ortiz-Gonzalez, P. N. Pichurin, J. Pinner, Z. Powis, C. Prasad, F. C. Radio, K. J. Rasmussen, D. L. Renaud, E. T. Rush, C. Saunders, D. Selcen, A. R. Seman, D. N. Shinde, E. D. Smith, T. Smol, L. S. Blok, J. M. Stoler, S. Tang, M. Tartaglia, M. L. Thompson, J. M. van de Kamp, J. Wang, D. Weise, K. Weiss, R. Woitschach, B. Wollnik, H. Yan, E. H. Zackaj, G. Zampino, P. Campeau, E. Bhoj, A second cohort of *CHD3* patients expands the molecular mechanisms known to cause Snijders Blok-Campeau syndrome. *Eur. J. Hum. Genet.* **28**, 1422–1431 (2020).
 51. E. A. Mannino, H. Miyawaki, G. Santen, S. A. Schrier Vergano, First data from a parent-reported registry of 81 individuals with Coffin-Siris syndrome: Natural history and management recommendations. *Am. J. Med. Genet. A* **176**, 2250–2258 (2018).
 52. O. R. Homann, K. Misura, E. Lamas, R. W. Sandrock, P. Nelson, S. I. McDonough, L. E. DeLisi, Whole-genome sequencing in multiplex families with psychoses reveals mutations in the *SHANK2* and *SMARCA1* genes segregating with illness. *Mol. Psychiatry* **21**, 1690–1695 (2016).
 53. E.-M. Strehle, L. Yu, J. A. Rosenfeld, S. Donkervoort, Y. Zhou, T.-J. Chen, J. E. Martinez, Y.-S. Fan, D. Barbooth, H. Zhu, A. Vaglio, R. Smith, C. A. Stevens, C. J. Curry, R. L. Ladda, Z. J. Fan, J. E. Fox, J. A. Martin, H. Z. Abdel-Hamid, E. A. McCracken, B. C. McGillivray, D. Masser-Frye, T. Huang, Genotype-phenotype analysis of 4q deletion syndrome: Proposal of a critical region. *Am. J. Med. Genet. A* **158A**, 2139–2151 (2012).
 54. B. Duga, M. Czako, K. Komlosi, K. Hadzsiev, K. Torok, K. Sumegei, P. Kisfali, G. Kosztolanyi, B. Melegh, Deletion of 4q28.3-31.23 in the background of multiple malformations with pulmonary hypertension. *Mol. Cytogenet.* **7**, 36 (2014).
 55. J. H. Rim, S. W. Kim, S.-H. Han, J. Yoo, Clinical and molecular delineation of a novel de novo 4q28.3-31.21 interstitial deletion in a patient with developmental delay. *Yonsei Med. J.* **56**, 1742–1744 (2015).
 56. G. W. E. Santen, E. Aten, A. T. Vulto-van Silfhout, C. Pottinger, B. W. M. van Bon, I. J. H. M. van Minderhout, R. Snowdowne, C. A. C. van der Lans, M. Boogaard, M. M. L. Linssen, L. Vijffhuizen, M. J. R. van der Wielen, M. J. E. Vollebregt, Coffin-Siris

- Consortium, M. H. Breuning, M. Kriek, A. van Haeringen, J. T. den Dunnen, A. Hoischen, J. Clayton-Smith, B. B. A. de Vries, R. C. M. Hennekam, M. J. van Belzen, Coffin-Siris syndrome and the BAF complex: Genotype-phenotype study in 63 patients. *Hum. Mutat.* **34**, 1519–1528 (2013).
57. G. Cappuccio, C. Sayou, P. L. Tanno, E. Tisserant, A.-L. Bruel, S. E. Kennani, J. Sá, K. J. Low, C. Dias, M. Havlovicová, M. Hančárová, E. E. Eichler, F. Devillard, S. Moutton, J. Van-Gils, C. Dubourg, S. Odent, B. Gerard, A. Piton, T. Yamamoto, N. Okamoto, H. Firth, K. Metcalfe, A. Moh, K. A. Chapman, E. Aref-Eshghi, J. Kerkhof, A. Torella, V. Nigro, L. Perrin, J. Piard, G. L. Guyader, T. Jouan, C. Thauvin-Robinet, Y. Duffourd, J. K. George-Abraham, C. A. Buchanan, D. Williams, U. Kini, K. Wilson; Telethon Undiagnosed Diseases Program, S. B. Sousa, R. C. M. Hennekam, B. Sadikovic, J. Thevenon, J. Govin, A. Vitobello, N. Brunetti-Pierri, De novo *SMARCA2* variants clustered outside the helicase domain cause a new recognizable syndrome with intellectual disability and blepharophimosis distinct from Nicolaides-Baraitser syndrome. *Genet. Med.* **22**, 1838–1850 (2020).
58. M. Alvarez-Saavedra, K. Yan, Y. De Repentigny, L. E. Hashem, N. Chaudary, S. Sarwar, D. Yang, I. Ioshikhes, R. Kothary, T. Hirayama, T. Yagi, D. J. Picketts, *Snf2h* drives chromatin remodeling to prime upper layer cortical neuron development. *Front. Mol. Neurosci.* **12**, 243 (2019).
59. R. Xi, T. Xie, Stem cell self-renewal controlled by chromatin remodeling factors. *Science* **310**, 1487–1489 (2005).
60. C. Han, L. Y. Jan, Y.-N. Jan, Enhancer-driven membrane markers for analysis of nonautonomous mechanisms reveal neuron-glia interactions in *Drosophila*. *Proc. Natl. Acad. Sci. U.S.A.* **108**, 9673–9678 (2011).
61. Y. Song, D. Li, O. Farrelly, L. Miles, F. Li, S. E. Kim, T. Y. Lo, F. Wang, T. Li, K. L. Thompson-Peer, J. Gong, S. E. Murthy, B. Coste, N. Yakubovich, A. Patapoutian, Y. Xiang, P. Rompolas, L. Y. Jan, Y. N. Jan, The mechanosensitive ion channel *piezo* inhibits axon regeneration. *Neuron* **102**, 373–389.e6 (2019).
62. Y. O. Ali, W. Escala, K. Ruan, R. G. Zhai, Assaying locomotor, learning, and memory deficits in *Drosophila* models of neurodegeneration. *J. Vis. Exp.* **11**, 2504 (2011).
- Institute. The research conducted at the Murdoch Children's Research Institute was supported by the Victorian Government's Operational Infrastructure Support Program. Sequencing and analysis of individual 2 were provided by the Broad Institute of MIT and Harvard Center for Mendelian Genomics (Broad CMG) and were funded by the National Human Genome Research Institute, the National Eye Institute, and the National Heart, Lung, and Blood Institute (grant UM1 HG008900) and, in part, by National Human Genome Research Institute grant R01 HG009141. The DDD study presents independent research commissioned by the Health Innovation Challenge Fund (grant HICF-1009-003), a parallel funding partnership between Wellcome and the Department of Health, and the Wellcome Sanger Institute (grant WT098051). The views expressed in this publication are those of the author(s) and not necessarily those of Wellcome or the Department of Health. The study has UK Research Ethics Committee approval (10/H0305/83, granted by the Cambridge South REC, and GEN/284/12, granted by the Republic of Ireland REC). The research team acknowledges the support of the National Institute for Health Research through the Comprehensive Clinical Research Network.
- Author contributions:** D.L., A.K., H.B.F., M.B., M.J.G.S., E.W., E.J.B., M.J.M.N., C.G.-J., M.M., A.D.-W., H.L., J.A.M.-A., L.S.P., S.M.W., J.C., and H.H. contributed to the molecular evaluation of the affected individuals. N.B., K.G., E.W., J.H., M.J.M.N., A.S., D. Bartholomew, Y.H., E.M.C.S., T.B., D.C., D. Brown, K.L., T.G., D.T., T.Y.T., and M.A.D. contributed to the clinical evaluation of the affected individuals. D.L., Q.W., N.N.G., M.E.M., M.S.K., and Y.S. contributed to the functional investigations. All authors read, edited, and approved the manuscript. **Competing interests:** K.M. and M.J.G.S. are employees of GeneDx Inc. C.G.-J. is an employee of Regeneron. The authors declare no other competing interests. **Data and materials availability:** Patient variants are available in the Leiden Open Variation Database (LOVD; www.LOVD.nl/SMARCA5). All data needed to evaluate the conclusions in the paper are present in the paper and/or the Supplementary Materials. Additional data related to this paper may be requested from the authors.

Submitted 14 October 2020

Accepted 23 March 2021

Published 12 May 2021

10.1126/sciadv.abf2066

Acknowledgments: We thank all of the families involved in this study for their participation. **Funding:** Research reported in this publication was supported, in part, by the Roberts Collaborative Functional Genomics Rapid Grant (to D.L. and M.A.D.) from CHOP and Institutional Development Funds (to H.H.) from CHOP. This work was supported by NIH grants DP2 NS111996 (to M.S.K.) and T32 HL07953 (to N.N.G.) and funding from the Burroughs Wellcome Fund (to M.S.K.). We are grateful for funding support for the Undiagnosed Diseases Program Victoria from the Harbig Family Foundation and the Murdoch Children's Research

Citation: D. Li, Q. Wang, N. N. Gong, A. Kurolap, H. B. Feldman, N. Boy, M. Brugger, K. Grand, K. McWalter, M. J. Guillen Sacoto, E. Wakeling, J. Hurst, M. E. March, E. J. Bhoj, M. J. M. Nowaczyk, C. Gonzaga-Jauregui, M. Mathew, A. Dava-Wala, A. Siemon, D. Bartholomew, Y. Huang, H. Lee, J. A. Martinez-Agosto, E. M. C. Schwaibold, T. Brunet, D. Choukair, L. S. Pais, S. M. White, J. Christodoulou, D. Brown, K. Lindstrom, T. Grebe, D. Tiosano, M. S. Kayser, T. Y. Tan, M. A. Deardorff, Y. Song, H. Hakonarson, Pathogenic variants in *SMARCA5*, a chromatin remodeler, cause a range of syndromic neurodevelopmental features. *Sci. Adv.* **7**, eabf2066 (2021).

Pathogenic variants in *SMARCA5*, a chromatin remodeler, cause a range of syndromic neurodevelopmental features

Dong LiQin WangNaihua N. GongAlina KurolapHagit Baris FeldmanNikolas BoyMelanie BruggerKatheryn GrandKirsty McWalterMaria J. Guillen SacotoEmma WakelingJane HurstMichael E. MarchElizabeth J. BhojMa#gorzata J. M. NowaczykClaudia Gonzaga-JaureguiMariam MathewAshita Dava-WalaAmy SiemonDennis BartholomewYue HuangHane LeeJulian A. Martinez-AgostoEva M. C. SchwaiboldTheresa BrunetDaniela ChoukairLynn S. PaisSusan M. WhiteJohn ChristodoulouDana BrownKristin LindstromTheresa GrebeDov TiosanoMatthew S. KayserTiong Yang TanMatthew A. DeardorffYuanquan SongHakon Hakonarson

Sci. Adv., 7 (20), eabf2066. • DOI: 10.1126/sciadv.abf2066

View the article online

<https://www.science.org/doi/10.1126/sciadv.abf2066>

Permissions

<https://www.science.org/help/reprints-and-permissions>

Use of think article is subject to the [Terms of service](#)